Galectin-4 and sulfatides in apical membrane trafficking in enterocyte-like cells

Delphine Delacour,[1] Valérie Gouyer,[1] Jean-Pierre Zanetta,[2] Hervé Drobecq,[3] Emmanuelle Leteurtre,[1] Georges Grard,[4] Odile Moreau-Hannedouche,[1] Emmanuel Maes,[2] Alexandre Pons,[2] Sabine André,[5] André Le Bivic,[6] Hans Joachim Gabius,[5] Aki Manninen,[7] Kai Simons,[7] and Guillemette Huet[1]

[1]Unité INSERM 560, 59045 Lille Cedex, France
[2]UMR CNRS 8576, Unité de Glycobiologie Structurale et Fonctionnelle, 59655 Villeneuve d'Ascq, France
[3]UMR CNRS 8525, Institut de Biologie et Institut Pasteur de Lille, 59021 Lille, France
[4]Laboratoire de Biochimie, Hôpital Claude Huriez, 59045 Lille Cedex, France
[5]Institute of Physiological Chemistry, Faculty of Veterinary Medicine, Ludwig Maximilians University, D-80539 Munchen, Germany
[6]Laboratoire de Neurogenese et Morphogenese au cours du Developpement et chez l'Adulte (NMDA)/Institut de Biologie du Developpement de Marseille/IBDM, Case 907, Faculté des Sciences de Luminy, 13288 Marseille Cedex 09, France
[7]Max-Planck Institute of Molecular Cell Biology and Genetics, D-01307 Dresden, Germany

We have previously reported that 1-benzyl-2-acetamido-2-deoxy-α-D-galactopyranoside (GalNAcα-*O*-bn), an inhibitor of glycosylation, perturbed apical biosynthetic trafficking in polarized HT-29 cells suggesting an involvement of a lectin-based mechanism. Here, we have identified galectin-4 as one of the major components of detergent-resistant membranes (DRMs) isolated from HT-29 5M12 cells. Galectin-4 was also found in post-Golgi carrier vesicles. The functional role of galectin-4 in polarized trafficking in HT-29 5M12 cells was studied by using a retrovirus-mediated RNA interference. In galectin-4–depleted HT-29 5M12 cells apical membrane markers accumulated intracellularly. In contrast, basolateral membrane markers were not affected. Moreover, galectin-4 depletion altered the DRM association characteristics of apical proteins. Sulfatides with long chain-hydroxylated fatty acids, which were also enriched in DRMs, were identified as high-affinity ligands for galectin-4. Together, our data propose that interaction between galectin-4 and sulfatides plays a functional role in the clustering of lipid rafts for apical delivery.

Introduction

Epithelial cells contain two distinct surfaces with different composition and function. This polarity implies a strict regulation of the targeting of components to each surface of the cell (Mostov et al., 2000). Sorting of proteins toward the basolateral membrane is encoded by tyrosine or di-leucine–based motifs, localized in the cytoplasmic domain (Matter and Mellman, 1994). These sorting motifs are recognized by adaptor complexes (APs; Nakatsu and Ohno, 2003). An AP complex (AP-1B) specifically expressed in epithelial cells is involved in sorting to the basolateral membrane (Folsch et al., 1999).

Correspondence to Guillemette Huet: huet@lille.inserm.fr

Abbreviations used in this paper: 2-D, 2-dimensional; AP, adaptor complex; CEA, carcinoembryonic antigen; CRD, carbohydrate recognition domain; DPP-IV, dipeptidylpeptidase-IV; DRM, detergent-resistant membrane; FAMEs, fatty-acid methyl esters; GalNAcα-*O*-bn, 1-benzyl-2-acetamido-2-deoxy-α-D-galactopyranoside; GC-MS, gas chromatography mass spectrometry; HPTLC, high performance thin layer chromatography; KD, knockdown; MALDI-TOF, matrix-assisted laser desorption/ionization–time of flight; RNAi, RNA interference; ST3Gal I, CMP-NeuAc: Galβ1-3GalNAc α2,3-sialyltransferase.

The online version of this article contains supplemental material.

The apical delivery has been proposed to involve the recruitment of apical glycoproteins into lipid rafts, which would then bud from the TGN to form apical carrier vesicles (Simons and Ikonen, 1997; Schuck and Simons, 2004). Rafts are membrane microdomains enriched in sphingolipids and cholesterol. Raft association plays a role in sorting to the apical surface (Brown and Rose, 1992; Lipardi et al., 2000; Alfalah et al., 2002). However, this association is not sufficient for apical delivery (Benting et al., 1999). At present, the signals and mechanisms by which proteins are specifically targeted to the apical surface are not fully understood. Involvement of N- and/or O-linked glycans was documented by studies using mutation, deletion or addition of glycosylation sites, or using drugs affecting the processing of oligosaccharide chains (Scheiffele et al., 1995; Yeaman et al., 1997; Gut et al., 1998; Huet et al., 1998; Monlauzeur et al., 1998; Alfalah et al., 1999, 2002; Benting et al., 1999; Jacob et al., 2000). VIP36, a lectin identified as a component of isolated carrier vesicles, has been implicated in sorting of proteins for apical delivery (Fiedler and Simons, 1996).

The Journal of Cell Biology, Vol. 169, No. 3, May 9, 2005 491–501
http://www.jcb.org/cgi/doi/10.1083/jcb.200407073

However, subsequent studies reported that VIP36 cycles in the early secretory pathway without moving beyond the Golgi complex thereby challenging the role of this lectin in apical sorting (Füllekrug et al., 1999; Hara-Kuge et al., 2004).

A role for glycosylation in apical transport was further supported by our observations that biosynthetic transport of apical but not basolateral glycoproteins was perturbed in 1-benzyl-2-acetamido-2-deoxy-α-D-galactopyranoside (GalNAcα-*O*-bn)–treated HT-29 cells (Huet et al., 1998; Gouyer et al., 2001). GalNAcα-*O*-bn is thought to function as a competitive inhibitor of the elongation of *N*-acetylgalactosamine, the first sugar residue in O-linked glycans. However, not only *O*-glycosylated glycoproteins but also *N*-glycosylated proteins as well as proteins implicated in regulation of apical traffic accumulated intracellularly in GalNAcα-*O*-bn–treated HT-29 cells (Delacour et al., 2003). GalNAcα-*O*-bn is extensively metabolized in HT-29 cells and could, thus, also interfere with other glycosylation processes than the *O*-glycosylation (Delannoy et al., 1996; Zanetta et al., 2000).

Based on these results, we have now investigated whether a lipid raft-based lectin-dependent mechanism of apical targeting could be operating in epithelial HT-29 cells.

Results

To identify proteins possibly associated with lipid rafts in HT-29 5M12 we used 2-dimensional (2-D) electrophoresis and matrix-assisted laser desorption/ionization–time of flight (MALDI-TOF) mass spectrometry analysis of detergent-resistant membrane fractions (DRMs).

Galectin-4 is a major component of DRMs in HT-29 5M12 cells

The 2-D gel electrophoresis pattern of DRMs is shown in Fig. 1, and the identity of corresponding proteins in Table I. Besides flotillin-1, an ubiquitous marker of DRMs, the proteins identified could be divided into eight groups: (1) G proteins (G(i) α1,2,3, G11, GTPase-activating protein for Rab6); (2) proteins of SNARE machinery (NSF, SNAP23); (3) proteins of vesicular structures (Rab22a, annexin II); (4) chaperone proteins (heat-shock protein 90 (hsp90), BiP, endoplasmin, hsp73); (5) ionic pumps (V-ATPase, voltage-dependent anion channel 2); (6) membrane cytoskeleton and intermediate filament-associated proteins (αII-spectrin, α4-actinin, myosin light chain, periplakin, mitofilin, cytokeratins 8, 18, 19, and 20); (7) apical membrane glycoproteins dipeptidylpeptidase-IV (DPP-IV), carcinoembryonic antigen (CEA), nonspecific cross-reacting antigen, 5′-nucleotidase, CD59); and (8) a member of the galectin family of lectins, galectin-4. Proteins of the three latter groups were the major proteins of the DRMs.

GalNAcα-*O*-bn decreases the amount of galectin-4 associated with DRMs

Prompted by the hypothesis of a role for glycans in apical transport, we analyzed whether galectin-4 was present in DRMs in GalNAcα-*O*-bn–treated cells. The 2-D gel electrophoresis protein pattern of DRMs of GalNAcα-*O*-bn–treated

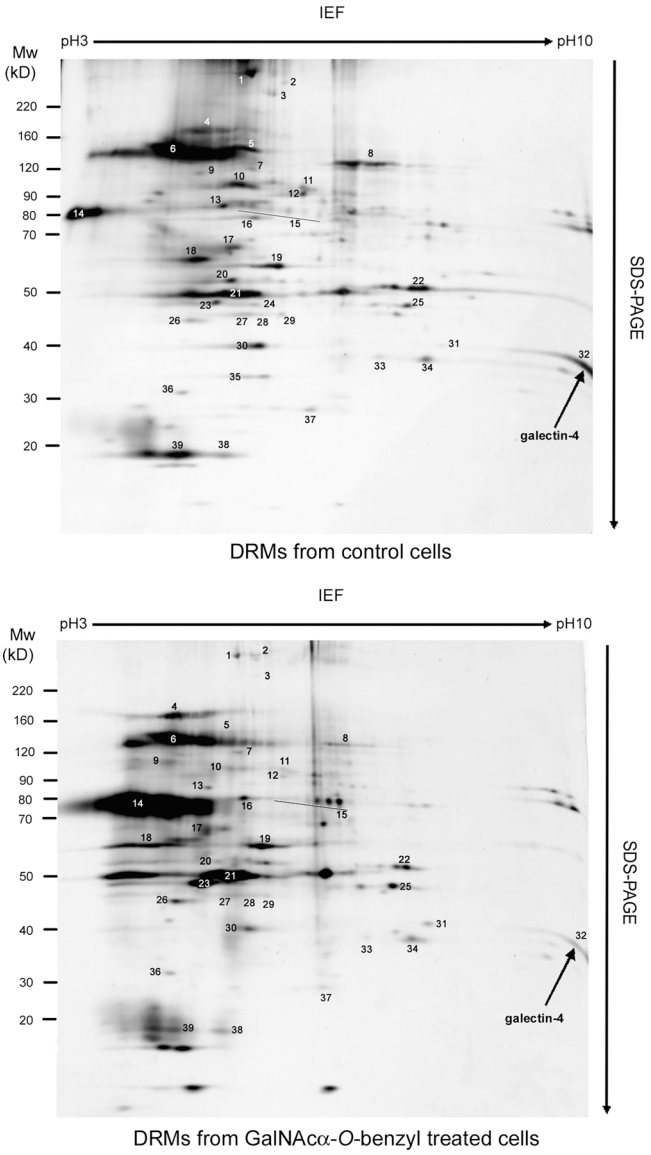

Figure 1. **Analysis of proteins contained in DRMs of control and GalNAcα-*O*-bn–treated HT-29 cells.** 2-D patterns were obtained using 300 μg of DRM proteins isolated from control and GalNAcα-*O*-bn–treated (14 d) cells. Each protein spot was numbered and submitted to mass spectrometry analysis in MALDI-TOF mode. Spot number 32 was identified as galectin-4 (arrows).

cells was similar to that of control cells (Fig. 1). Marked qualitative and/or quantitative changes were observed for a number of proteins. Interestingly, the levels of galectin-4 in DRMs were strongly decreased in GalNAcα-*O*-bn–treated cells, pointing to an effect of GalNAcα-*O*-bn on the interaction of galectin-4 with raft-associated compounds.

GalNAcα-*O*-bn modifies the cellular distribution of galectin-4

The distribution of galectin-4 in control and in GalNAcα-*O*-bn–treated cells was studied by analyzing the culture medium, the cytosolic and the total membrane fractions from saponin-permeabilized cells for the presence of galectin-4 (Fig. 2 A). In control cells, galectin-4 was found in the membrane fraction,

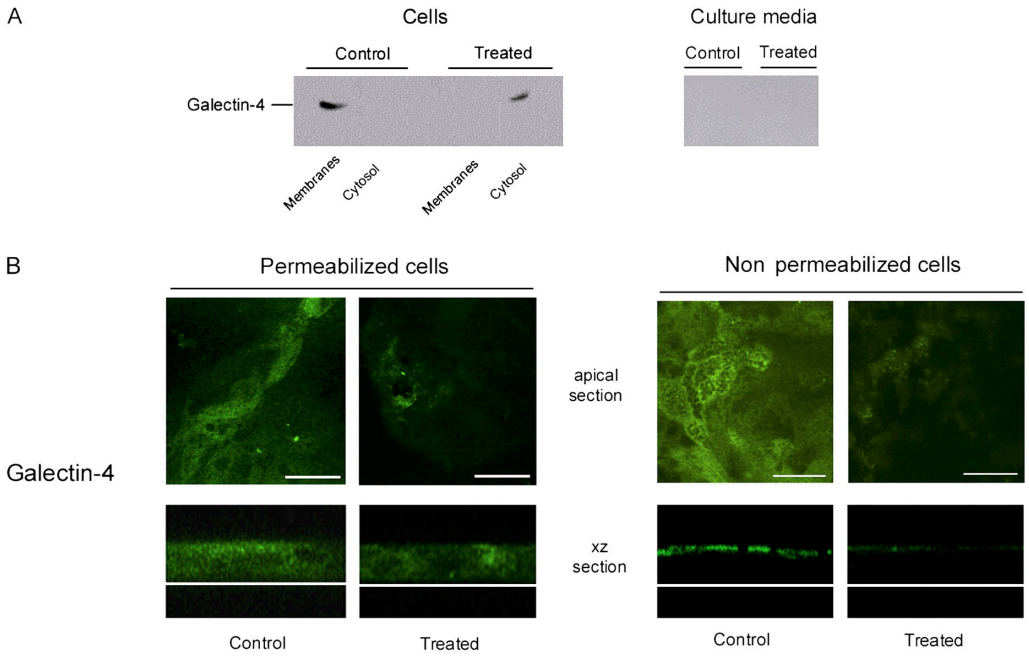

Figure 2. **GalNAcα-*O*-bn decreases the apical localization of galectin-4.** (A) Western blot of culture media, cytosol and membrane fractions of control and GalNAcα-*O*-bn–treated (14 d) cells after permeabilization with saponin, using anti–galectin-4 antibody. (B) Confocal microscopy with an anti–galectin-4 antibody on permeabilized or unpermeabilized control and GalNAcα-*O*-bn–treated (14 d) cells. Apical and xz sections are shown. Bars, 22 μm.

whereas in GalNAcα-*O*-bn–treated cells, galectin-4 was found in the soluble cytosolic fraction. Neither the control cells nor the GalNAcα-*O*-bn–treated cells secreted detectable levels of galectin-4 to the culture medium.

Confocal microscopy on permeabilized cells showed that galectin-4 was distributed throughout the cytoplasm, but mostly in the subapical region (Fig. 2 B). Furthermore, immunostaining on nonpermeabilized cells revealed the presence of galectin-4 at the extracellular surface of the apical membrane. This extracellular galectin-4 staining disappeared if cells were treated with trypsin from the outside (unpublished data). In permeabilized GalNAcα-*O*-bn–treated cells accumulation of galectin-4 in the subapical region was no longer observed (Fig. 2 B). Moreover, a clear decrease in the extracellular fraction of galectin-4 at the apical membrane was observed in GalNAcα-*O*-bn–treated, nonpermeabilized cells (Fig. 2 B).

Galectin-4 is associated with DRMs in post-Golgi carrier vesicle preparations

We then proceeded to analyze whether galectin-4 was present in membrane vesicles released from perforated HT-29 cells (Wandinger-Ness et al., 1990). Immunoelectron microscopy demonstrated that galectin-4 was in carrier vesicles containing DPP-IV (Fig. 3 A).

To determine whether galectin-4 was localized on the lumenal or cytoplasmic side of these vesicles, we subjected the vesicle preparations to trypsin. Galectin-4 was not sensitive to trypsin, suggesting that the lectin was localized on the lumenal side of post-Golgi vesicles (Fig. 3 B). Galectin-4 in these preparations became susceptible to trypsin upon addition of detergent (Fig. 3 B).

Galectin-4 has been previously described as an intestinal brush border protein with potential functions as a raft stabilizer/organizer characterized by insolubility in Triton X-100 at 37°C ("super-rafts"; Danielsen and van Deurs, 1997; Braccia et al., 2003). We therefore examined the DRM association of galectin-4 in isolated post-Golgi vesicles of HT-29 5M12 cells using the two-step procedure described by Braccia et al. (2003). Vesicle preparations were treated by 1% Triton X-100 at 4°C, fractionated into supernatant (S) and pellet; the pellet was resuspended into Triton X-100, incubated at 37°C and then further fractionated into supernatant (P1) and pellet (P2). Galectin-4 was only present in P2, i.e., the detergent-insoluble fraction at 37°C (Fig. 3 C). DPP-IV was similarly detected only in the Triton X-100–insoluble fraction at 37°C. Annexin XIIIb and XIIIa were partially Triton X-100 soluble at 4°C but their DRM fraction remained insoluble at 37°C (particularly for annexin XIIIb).

GalNAcα-*O*-bn treatment decreases the amount of glycosphingolipids in DRMs of HT-29 5M12 cells

We then investigated the effect of GalNAcα-*O*-bn on the lipid composition of the DRMs using a quantitative analysis by high performance thin layer chromatography (HPTLC) and gas chromatography mass spectrometry (GC-MS) in reference to the total membrane fraction. Results in control cells demonstrated enrichment of glycosphingolipids (from 12.16% in total membrane preparation to 34.90% in total DRM preparation) and cholesterol (from 22.78 to 35.13% in DRMs). Sphingomyelin was barely detectable. Among the glycosphingolipids, galactosyl-ceramides were the major class (51.18%), followed by

Table I. **Identification of common protein components in DRMs from control and GalNAcα-*O*-benzyl–treated HT-29 5M12 cells**

Spot no.	Identity	Accession no.	Protein parameters		MALDI-TOF MS	
			MW (kD)	pI	Matched peptides	Sequence coverage
1	Spectrin, non-erythroid α chain, α-II spectrin, fodrin α chain	Q13813	285,85	5,2	45	22%
2	Periplakin	O60437	204,65	5,44	19	15%
3	Clathrin heavy chain	Q00610	193,37	5,5	9	8%
4	Carcinoembryonic antigen (CEA)	P06731	76,79	5,43	3	7%
5	Integrin alpha chain, alpha 6	P23229	126,62	6,39	9	13%
6	Dipeptidylpeptidase IV (cd26, adenosine desaminase complexing protein 2)	P27487	88,27	5,67	16	23%
7	α-Actinin 4 (F-actin cross linking protein)	O43707	104,85	5,27	28	33%
8	Vesicular-fusion protein NSF (*N*-ethylmaleimide–sensitive fusion protein) (NEM-sensitive protein)	P46459	82,65	6,38	5	8%
9	Endoplasmin precursor (94-kD glucose-regulated protein) (GRP94)	P14625	92,47	4,76	10	18%
10	Heat shock protein 90-kD (hsp90)	P07900	84,54	4,94	7	16%
11	Junction plakoglobin	P14923	81,49	5,95	23	38%
12	Mitofilin	Q16891	79,86	5,7	23	34%
13	BiP	P11021	72,33	5,07	18	34%
14	Carcinoembryonic antigen-related cell adhesion molecule 6 precursor, normal cross-reacting antigen, nonspecific cross-reacting antigen (NCA) CD66c	P40199	37,24	5,56	3	8%
15	CD73 (5′-nucleotidase)	P21589	63,36	6,58	7	18%
16	Heat shock cognate 71-kD protein (hsc71) (hsp73)	P11142	70,89	5,37	14	27%
17	Vacuolar ATP synthase subunit B (V-ATPase B subunit)	P15313	56,98	5,52	11	28%
18	Keratin 9, type I cytoskeletal	P35527	61,98	5,14	17	46%
19	Keratin 8, type II cytoskeletal	P05787	53,54	5,52	21	37%
20	Keratin 20, type I cytoskeletal	P35900	48,48	5,52	11	31%
21	Keratin 18, type I cytoskeletal	P05783	53,54	5,52	21	37%
22	Flotillin-1	O75955	47,33	7,04	8	26%
23	Keratin 19, type I cytoskeletal	P08727	44,1	5,05	28	65%
24	Protein G11	P29992	42,12	5,51	4	16%
25	Vacuolar ATP synthase subunit C (V-ATPase C subunit)	P21283	43,94	7,02	37	22%
26	Vacuolar ATP synthase subunit D (V-ATPase D subunit)	P12953	40,33	4,89	7	22%
27	Guanine nucleotide-binding protein α-I subunit (G(i) α2)	P04899	41	5,3	5	20%
28	Guanine nucleotide-binding protein α-I subunit (G(i) α3)	P08754	41,08	5,5	5	19%
29	Guanine nucleotide-binding protein α-I subunit (G(i) α1)	P04898	40,91	5,7	6	21%
30	Guanine nucleotide-binding regulatory protein-β-2 subunit, transducin β-2 subunit (Gβ2)	P11016	37,33	5,6	14	49%
31	Annexin II (lipocortin II) (calpactin I heavy chain)	P07355	38,47	7,56	13	35%
32	Galectin-4; lectin galactoside-binding soluble 4	P56470	35,94	9,21	9	39%
33	Voltage-dependent anion channel 2 (VDCA2)		32,09	7,7	6	35%
34	Ras-related protein Rab-22A	Q9UL26	21,85	8,32	4	35%
35	Prohibitin	P35232	29,84	5,6	6	30%
36	Synaptosomal-associated protein 23 (SNAP-23) (vesicle-membrane fusion protein SNAP-23)	O00161	23,35	4,89	6	34%
37	Rab6 GTPase activating protein, GAPCenA	Q9Y3P9	23,56	5,4	6	9%
38	CD59 (protectin)	P13987	14,17	6,02	3	26%
39	Myosin light chain, non-muscle isoform	P16475	17,08	4,6	10	54%

Spot proteins are numbered on 2-D gels in Fig. 1 A. The SWISS-PROT and TREMBL accession nos. are listed. Theorical molecular masse, isoeletric point, number of matched peptides, and sequence coverage obtained along the searches in databases are presented. Spectra were acquired by MALDI-TOF mass spectrometry. Searches in databases were done by using the Profound software.

sulfatides (33.05%), GM3 (12.98%), and GM1 (2.79%; Table II). Fatty-acid methyl esters (FAMEs) analysis revealed that DRMs were enriched in hydroxylated fatty acids (all hydroxylated in position 2 with a predominance of the C24:0 chain; 11.36% vs. 0.32% in total membranes).

When DRMs were prepared from cells treated with GalNAcα-*O*-bn the amount of cholesterol increased by twofold (54.56% vs. 35.13% in control cells), whereas the amount of glycosphingolipids was decreased by twofold (16.50% vs. 34.90% in control cells; Table II). FAMEs analysis showed a decrease in hydroxylated C24:0 (7.58% vs. 11.36% in control cells), with a simultaneous increase in mono-unsaturated FAMEs (C16:1 and C18:1). These changes after GalNAcα-*O*-bn treatment prompted us to look for galactosylated glycosphingolipids as ligands for galectin-4.

Identification of glycosphingolipids as carbohydrate ligands of galectin-4

Galectin-4 immunoprecipitates were analyzed by HPTLC (Fig. 4 A), GC-MS, and MALDI-TOF mass spectrometry. In control

Table II. **Lipid analysis of total membranes and DRMs**

Control cells								
Sugars	**Total membranes**	**Total DRMs**	**FAMEs**	**Total membranes**	**Total DRMs**	**Lipids**	**Total membranes**	**Total DRMs**
Fuc	0.19	1.2	C14:0	2.14%	4.87%	Chol	22.78%	35.13%
Ins	0	1.08	C15:0	0.00%	1.51%			
Gal	7.66	16.16	C16:1	19.92%	1.61%	PL	65.06%	24.97%
Man	0	0.44	C16:0	18.08%	31.18%	PE	11.12%	25.53%
GalNAc	1	1	C16:0oh2	0.87%	3.28%	PI	0.25%	14.95%
GlcNAc	0	2.59	C18:1	45.05%	4.34%	PS	0.25%	37.74%
NeuAc	0.59	2.05	C18°:0	12.50%	31.96%	PC	88.39%	21.15%
Total	9.44	24.52	C22°:0	0.00%	1.98%			
			C22°:0oh2	0.79%	3.12%	GSL	12.16%	34.90%
LCBs			C23°:0oh2	0.32%	2.19%	Gce	6.30%	51.18%
Spha	26.04%	14.02%	C24°:1oh2	0.00%	1.62%	LacC	8.24%	ND
6ohSphe	32.23%	28.86%	C24°:0oh2	0.32%	11.36%	Sul	84.09%	33.05%
Sphe	23.13%	16.24%	C25°:0oh2	0.01%	0.62%	GM3	ND	12.98%
Phyt	18.60%	40.87%	C26°:0oh2	0.00%	0.35%	GM1	ND	2.79%
						GD1a	0.39%	ND
AAG			FAM/LCB	9.487	1.472	GD1b	ND	ND
C16:0	48.99%	68.22%	AAG°:LCB	1.106	0.079	GT1b	ND	ND
C18:1	29.70%	4.34%	Sugar/LCB	1.499	1.137			
C18:0	21.31%	31.78%	Gal+N/LCB	1.392	0.796	SM	ND	<5%
Treated cells								
Fuc	0.32	1.42	C14:0	3.35%	3.42%	Chol	22.57%	54.56%
Ins	3.19	1.72	C15:0	0.36%	0.97%			
Gal	9.25	17.71	C16:1	21.60%	5.06%	PL	64.86%	23.94%
Man	0	1.07	C16:0	18.81%	32.36%	PE	8.07%	25.69%
GalNAc	0	1	C16:0oh2	1.07%	2.46%	PI	2.80%	15.05%
GlcNAc	1	2.32	C18:1	40.28%	19.78%	PS	2.80%	37.98%
NeuAc	0.73	2.24	C18°:0	12.13%	21.79%	PC	83.33%	21.13%
Total	14.49	27.47	C22:0	1.44%	1.49%			
			C22°:0oh2	0.70%	2.22%	GSL	2.57%	16.50%
LCBs			C23°:0oh2	0.26%	1.13%	Gce	6.98%	39.11%
Spha	37.22%	12.41%	C24°:1oh2	0.00%	1.31%	LacC	ND	ND
6ohSphe	24.65%	29.47%	C24°:0oh2	0.00%	7.58%	Sul	93.03%	38.8%
Sphe	24.45%	24.84%	C25°:0oh2	0.00%	0.32%	GM3	ND	22.09%
Phyt	13.68%	33.27%	C26°:0oh2	0.00%	0.13%	GM1	ND	ND
						GD1a	ND	ND
AAG			FAM/LCB	9.087	2.425	GD1b	ND	ND
C16:0	0.00%	67.87%	AAG°:LCB	1.114	0.113	GT1b	ND	ND
C18:1	58.37%	19.78%	Sugar/LCB	2.976	1.422			
C18:0	41.63%	32.13%	Gal+N/LCB	2.167	0.968	SM	ND	<5%

Monosaccharides and inositol (Ins), FAMEs, long-chains bases (LCBs), and alkyl-acyl-glycerols (AAGs) were determined in single GC/MS experiments as the HFB derivatives of the constituents released using acid-catalyzed methanolysis. The relative molar proportion of cholesterol (Chol) and of phospholipids (PL) was determined by scanning the iodine stain of HPTLC plates. The relative molar proportions of glycosphingolipids (GSL) was determined by scanning the orcinol-sulfuric acid staining of HPTLC plates and the molar ratio of sialylated compounds relative to cerebrosides and sulfatides confirmed by GC/MS analysis. FAMEs hydroxylated in position 2 are termed as (Cn:0/1)oh2 where *n* = the no. of carbon atoms of the chain and 0/1 the no. of double bonds. PE, phosphatidylethanolamine; PI, phosphatidylinositol; PS, phosphatidylserine; PC, phosphatidylcholine; GalCer, galactosyl-ceramides; LacCer, lactosyl-ceramides. ND, not detected; Phyt, phytosphingosine; SM, sphingomyelin; Spha, sphinganine; 6ohSphe, 6-hydroxy-sphingosine; Sul, sulfatides. Results are expressed as molar ratio or percentage of molar ratio.

cells, galactosyl-ceramides and sulfatides were identified as major constituents. Gangliosides were not detected. The fatty acid composition showed a high content of 2-hydroxylated FAMEs with chain length of 18 or 22 to 26 carbon atoms (>50%; 24:0).

When similar experiments were performed on cells treated with GalNAcα-*O*-bn for 12 d, the quantity of material recovered was extremely low (<1% of the control cells) and not detectable by HPTLC, indicating a dramatic inhibition in the formation of glycosphingolipid–galectin-4 complexes (Fig. 4 A). A short time exposure to GalNAcα-*O*-bn (18 h) was also used and trace amounts of less polar sulfatides were recovered (~10% of the control).

To gain further insight into possible glycosphingolipids–galectin-4 interactions, we used human glycosphingolipid preparations from sciatic nerve, for overlay experiments with the recombinant NH_2- or COOH-terminal domains of galectin-4. Each of these domains contains one of the two carbohydrate recognition domains (CRDs) in galectin-4. A strong binding of both the NH_2-terminal and COOH-terminal domain of galectin-4 was observed to the more polar fraction of sulfatides, i.e., those substituted by 2-hydroxylated fatty acids (Fig. 4 B). In contrast,

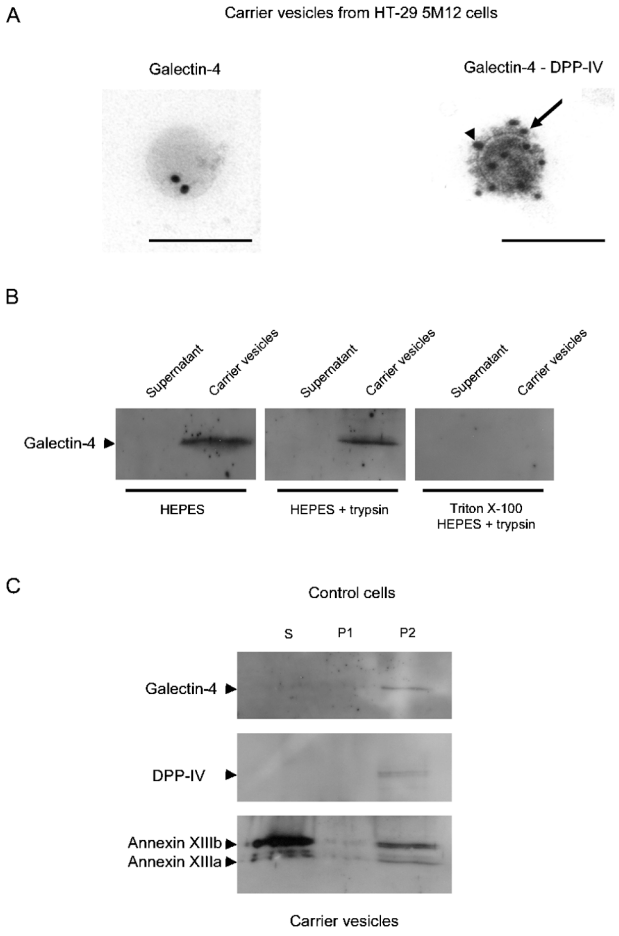

Figure 3. **Galectin-4 is associated with DRMs of post-Golgi carrier vesicles.** (A) Immunogold labeling of nascent carrier vesicles isolated from HT-29 5M12 cells. Galectin-4 (arrowhead) was labeled with 18-nm gold particles and DPP-IV (arrow) by 12-nm gold. Bars, 156 nm. In the vesicle preparation, 30% of the vesicles were labeled with the anti–DPP-IV antibody. 20% of these DPP-IV–positive vesicles were also labeled with galectin-4. (B) Western blotting of galectin-4 in carrier vesicles. Trypsin digestion of galectin-4 in untreated or Triton X-100–treated carrier vesicles is shown. (C) Detergent extractability of galectin-4, DPP-IV, and annexins XIIIb and XIIIa in carrier vesicles from HT-29 5M12 cells. Detergent extracts, i.e., Triton X-100 soluble (S), insoluble at 4°C but soluble at 37°C (P1), and insoluble at 37°C (P2), were analyzed by Western blotting.

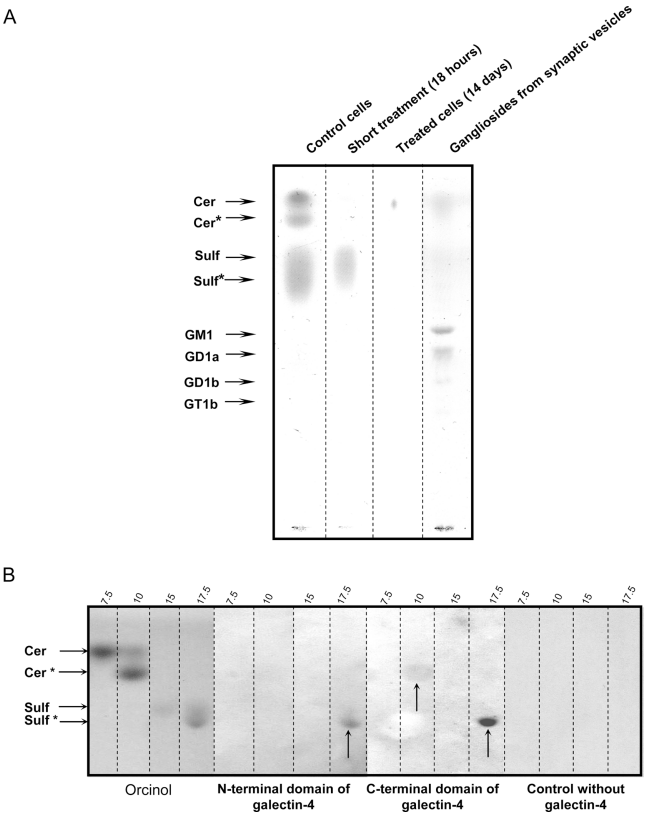

Figure 4. **Galectin-4 is no longer bound to sulfatides under GalNAcα-*O*-bn treatment.** (A) Co-immunoprecipitation of galectin-4 complexes and HPTLC analysis of glycolipid ligands. Co-immunoprecipitation was performed from the same quantity of control and GalNAcα-*O*-bn–treated (14 d and 18 h) cells. Plates were iodine stained and scanned. The material migrating as two bands of galactosylceramides (Cer and Cer*) and the trailing corresponding to sulfatides (Sulf and Sulf*) were recovered from the HPTLC plate, submitted to acid-catalyzed methanolysis and analyzed by GC-MS. Cer, sphinganine and nonhydroxylated fatty acids; Cer*, sphinganine and 2-hydroxylated fatty acids; Sulf and Sulf*, sphingosine, sphinganine, phytosphingosine and 6-hydroxy-sphingosine, and 2-hydroxylated fatty acids from 16 to 28 carbon atoms. (B) Overlay experiments on the four fractions corresponding to the galactosylceramides and sulfatides purified from human sciatic nerve. Fractions were identified by their eluting methanol percent. Their glycosphingolipids were visualized by orcinol staining and analyzed for binding to the NH_2-terminal CRD and the COOH-terminal CRD of galectin-4. Control without lectin is presented. arrows show the glycolipids which bind the NH_2-terminal or COOH-terminal domain of galectin-4.

the less polar sulfatides did not show any binding to the domains of galectin-4. In addition, a weak binding to the more polar galactosyl-ceramides was observed with the COOH-terminal domain of galectin-4. The addition of galactose (0.3 M) and lactose (0.1 M) during the incubation did not significantly reduce the binding of the two galectin-4 domains to the glycosphingolipids. No binding to gangliosides was observed (unpublished data).

The human sciatic nerve galectin-4 ligands were further characterized by GC-MS and MALDI-TOF mass spectrometry. Results showed that these ligands corresponded to sulfatides and galactosylceramides showing a similar composition as those identified after co-immunoprecipitation from HT-29 5M12 cells with the anti–galectin-4 antibody. By NMR spectroscopy, we demonstrated that galectin-4 ligands were β-galactosylceramides and 3-sulfated-β-galactosylceramide both containing 2-hydroxylated fatty acids (Fig. S1, available at http://www.jcb.org/cgi/content/full/jcb.200407073/DC1).

Sulfatides are found in DRMs, which are detergent insoluble at 37°C

To gain further insight into the role of these glycosphingolipid–galectin-4 complexes in detergent insolubility of raft microdomains, DRMs were first isolated from a total membrane preparation of control and GalNAcα-*O*-bn–treated cells using 1% Triton X-100 at 4°C. These DRMs, insoluble at 4°C, were then incubated at 37°C and both the soluble and the insoluble material (DRMs being detergent insoluble at 37°C) were examined by HPTLC (Fig. 5). The results showed the presence of galactosylceramides in all DRM fractions of control and GalNAcα-*O*-bn–treated cells, whereas sulfatides were

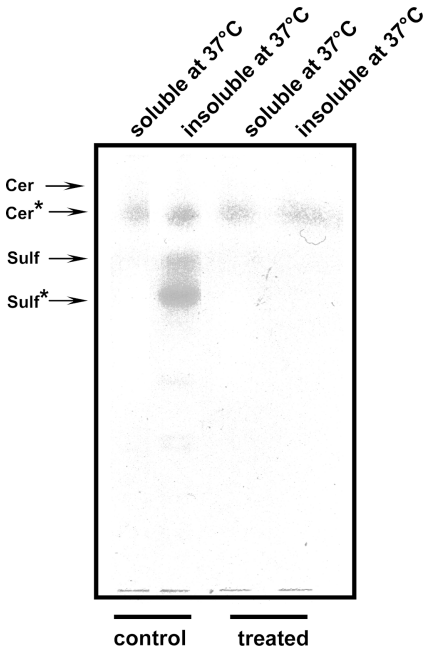

Figure 5. **Sulfatides are found in DRMs which are detergent insoluble at 37°C DRMs were isolated from a total membrane fraction of control and GalNAcα-*O*-bn–treated (14 d) cells.** DRMs were further warmed at 37°C and both the soluble and insoluble material were collected and examined by HPTLC.

only present in the DRM fraction detergent insoluble at 37°C in control cells.

Inhibition of galectin-4 expression abrogates apical targeting

To analyze whether galectin-4 had a role in the delivery of apical proteins, we depleted galectin-4 expression in HT-29 5M12 cells by RNA interference (RNAi). Galectin-4 RNAi constructs and controls are described in Fig. S2, available at http://www.jcb.org/cgi/content/full/jcb.200407073/DC1.

The level of galectin-4 mRNA depletion was analyzed by quantitative RT-PCR and Western blotting. The galectin-4 mRNA was reduced by 80% in the galectin-4-knockdown (KD) cell population and correlated well with the observed strong reduction (~80%) of the galectin-4 protein levels (Fig. 6 A).

We then analyzed the cellular localization of DPP-IV and two other apical markers, CEA, a glycosylphosphatidylinositol-anchored protein, and mucin (MUC1), a transmembrane protein, in the galectin-4-KD cells. In addition, localization of a basolateral marker, E-cadherin, was also studied. In the galectin-4-KD cells, the amount of DPP-IV, CEA, and MUC1 delivered to the apical membrane was significantly decreased (Fig. 6 B). Nevertheless, we did not observe mistargeting of DPP-IV, CEA, and MUC1 to the basolateral membrane upon galectin-4 depletion. Instead, we saw intracellular accumulation of these glycoproteins (Fig. 6 B). Costaining experiments with different organellar markers in galectin-4-KD cells showed partial colocalization of the cargo with lysosome-associated membrane protein 2 (not depicted). E-Cadherin localization was not altered in galectin-4-KD cells (Fig. 6 B). These results indicated that galectin-4 is required for efficient apical delivery of glycoproteins.

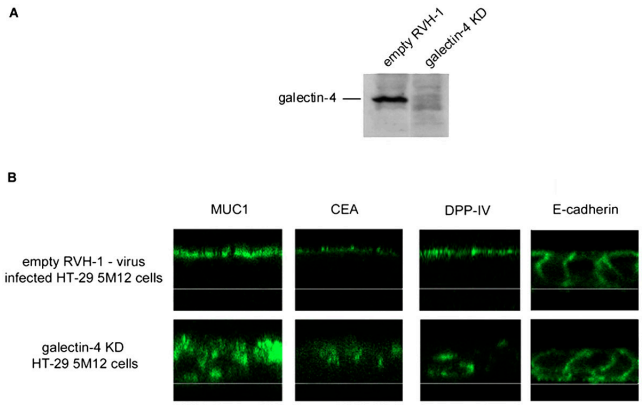

Figure 6. **KD of galectin-4 expression in HT-29 5M12 cells induces mistargeting of apical proteins.** (A) Western blot analysis of galectin-4 in empty-RVH-1-virus–infected cells or galectin-4-KD cells. (B) Confocal microscopy with antibodies directed against apical (MUC1, CEA, DPP-IV) and basolateral (E-cadherin) proteins, on empty-RVH-1-virus–infected cells or galectin-4 KD cells. xz sections are shown.

To determine whether galectin-4 depletion affected the organization of DRMs in HT-29 5M12 cells, we tested the detergent insolubility at 4 and 37°C of glycoproteins at the apical membrane on living cells. After Triton X-100 treatment of control cells at 37°C, apical staining of CEA and MUC1 and to some extent DPP-IV was still seen. In galectin-4-KD cells, CEA, MUC1, and DPP-IV were no longer detected after Triton X-100 extraction at 37°C (Fig. 7). We also examined the surface delivery of tsO45 VSVG, using basolateral and apical versions of this protein. The apical delivery was inhibited in the galectin-4-KD cells, whereas the basolateral VSV-G protein was transported normally to the basolateral membrane (Fig. S3, available at http://www.jcb.org/cgi/content/full/jcb.200407073/DC1).

Inhibition of galectin-4 expression decreases apical delivery of newly synthesized DPP-IV

To evaluate the impact of galectin-4 depletion on membrane trafficking to the apical or basolateral surfaces, the surface delivery of DPP-IV was studied using cell surface biotinylation. Chase times (4 and 6 h) were selected according to a previous study of the raft association of DPP-IV along its biosynthetic pathway in this cell type (Delacour et al., 2003). DPP-IV became detergent insoluble after 4 h. At this time, the maturation of the protein precursor into the mature glycosylated form was nearly complete and only the mature form was detergent insoluble. In galectin-4-KD cells, we observed a fourfold inhibition of DPP-IV delivery to the apical membrane (Fig. 8). Significant missorting of DPP-IV to the basolateral surface was not observed.

Discussion

Previous studies have shown that GalNAcα-*O*-bn inhibits the delivery of several apical proteins in HT-29 cells (Delacour et al., 2003). Because this inhibitor interferes with glycosylation it was appealing to assume that a lectin-based sorting mechanism was the basis for the inhibition. This paper demonstrates that

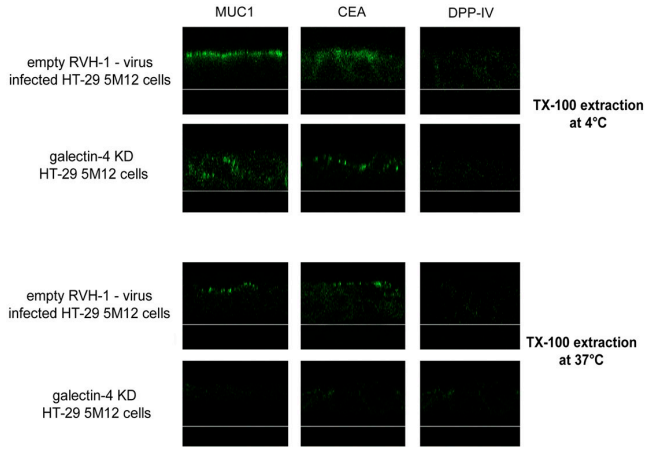

Figure 7. **Apical glycoproteins are no longer associated with DRMs in galectin-4-KD HT-29 5M12 cells.** Confocal microscopy with antibodies directed against MUC1, CEA, and DPP-IV, on empty-RVH-1-virus–infected cells or galectin-4-KD cells, after cell treatment with Triton X-100 at 4°C or 37°C. xz sections were shown.

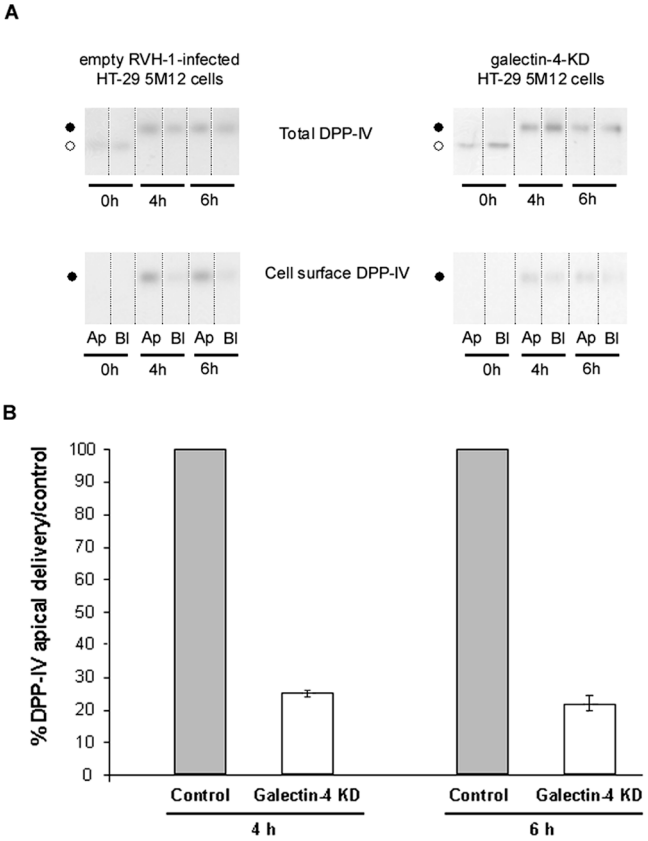

Figure 8. **Apical and basolateral delivery of DPP-IV in control and galectin-4-KD cells.** (A) Cells were pulse labeled for 30 min, and newly synthesized proteins were chased for 4 or 6 h and biotinylated from the apical or basolateral side. Aliquots from the immunoprecipitations (total) and streptavidin precipitations (cell surface) are shown. Ap, apical; Bl, basolateral. ○, DDP-IV precursor; ●, mature DPP-IV. (B) Apical and total DPP-IV signals were quantitated in control and in galectin-4-KD cells. The apical to total ratio in control cells was set to 100% and apical transport efficiency in galectin-4-KD cells is shown relative to this value. Data are means ± SD.

this could indeed be the case. We identified a lectin, galectin-4, as the main effector of GalNAcα-*O*-bn–mediated effects. This was based on several findings. First, galectin-4 is apically secreted in HT-29 cells. Second, it is a major constituent of DRMs in enterocytes and in HT-29 cells and could thus be part of a lectin-based raft clustering mechanism of apical delivery. Third, GalNAcα-*O*-bn treatment dramatically decreased the galectin-4 levels in DRMs. Fourth, the inhibitor also seemed to block the apical secretion of galectin-4. Finally and most importantly, silencing of galectin-4 expression using RNAi inhibited apical transport in the same way as previously shown to occur by GalNAcα-*O*-bn treatment in HT-29 cells. This is the first direct demonstration for a role of a lectin in apical transport.

Galectin-4 belongs to the galectin family of lectins, currently constituted of 15 individual members (Dunphy et al., 2002; Gray et al., 2004; Leffler et al., 2004). Galectin-4 is mostly expressed in the gastrointestinal tract of mammals. The HT-29 cells used in this study are derived from a colon adenocarcinoma. Galectin-4 is a monomer that contains two carbohydrate binding sites connected by a linker peptide (Oda et al., 1993). Galectin-4 has been shown to bind with high affinity to O-linked sulfoglycans (Ideo et al., 2002). The galectins function to form clusters, arrays or lattices through multivalent protein–carbohydrate interactions. These complexes can be a heterogeneous mixture of glycoprotein ligands but remarkably galectins can also selectively cross-link single glycoprotein species to form lectin-carbohydrate lattices (Fred Brewer, 2002). Galectins have been proposed to exert a multitude of functions, which is understandable considering that protein cross-linking plays an important role in cell signaling and membrane trafficking (Fred Brewer, 2002). Galectin-4 has been studied extensively in enterocytes by Danielsen and coworkers (Danielsen and van Deurs, 1997; Braccia et al., 2003). They have shown that galectin-4 forms what they call "super rafts" on the apical cell surface and in underlying structures such as deep apical tubules and subapical endocytic compartments (Braccia et al., 2003). These "super rafts" have the unusual property of being partially insoluble after Triton X-100 extraction at 37°C. One surprising property of galectins in the context of lectin-based sorting to the apical surface is the fact that these proteins do not possess signal peptides and do not use the normal secretory pathway over the Golgi complex to the cell surface (Hughes, 1999; Nickel, 2003). Instead, galectins accumulate in the cytosol and become externalized by an unknown mechanism. Where externalization occurs is also not known. This could take place at the plasma membrane or across cytoplasmic membrane organelles. Endosomes have been proposed but also translocation across the plasma membrane has been implicated (Hughes, 1999; Nickel, 2003).

We observed that GalNAcα-*O*-bn inhibited translocation of galectin-4 to the extracellular side of the apical plasma membrane. By confocal microscopy we could demonstrate that galectin-4 was normally localized throughout the cytosol and accumulated in the subapical region of the HT-29 cells. Immunostaining of unpermeabilized cells showed that galectin-4 was bound to the extracellular side of the apical membrane. After GalNAcα-*O*-bn treatment staining of galectin-4 disappeared from the apical surface and the subapical organelles. This was

also shown by fractionation experiments where galectin-4 was membrane-bound in control cells but became soluble after inhibitor treatment. How translocation of galectin-4 to the apical side is effected is not known. But because GalNAcα-*O*-bn treatment seemed to inhibit the process one could speculate that galectin ligands have to be present on the extracytoplasmic side of the translocation pore for transport across the membrane to occur. Several studies have analyzed which glycosylation processes GalNAcα-*O*-bn inhibits (Huang et al., 1992; Byrd et al., 1995; Delannoy et al., 1996; Huet et al., 1998). This seems to differ with cell type. In HT-29 cells GalNAcα-*O*-bn is converted into benzyldisaccharide Galβ1-3 GalNAcα-*O*-bn, which acts as a competitive inhibitor of CMP-NeuAc: Galβ1-3GalNAc α2,3-sialyltransferase (ST3Gal I), which is involved in the terminal elongation of O-linked glycans (Delannoy et al., 1996; Huet et al., 1998). However, other metabolites of the inhibitor were also formed, inhibiting other glycosylation enzymes (Zanetta et al., 2000). During this work we came up with a surprise. The major ligands of galectin-4 were found to be glycosphingolipids. Immunoprecipitation with anti–galectin-4 antibodies in a Triton X-100 and NP-40 mix at RT brought down galactosylceramides and sulfatides particularly enriched in long chain 2-hydroxylated fatty acids (50% of 2-hydroxylated; 24:0). The immunoprecipitates surprisingly contained few glycoproteins (unpublished data). By overlay assays we could confirm that recombinant NH_2- and COOH-terminal domains of galectin-4 bound preferentially to sulfatides substituted by 2-hydroxylated fatty acids and to a lesser extent to galactosylceramides similarly substituted. The 2-hydroxyl group of the long-chain fatty acids of galactosyl-ceramides and sulfatides is involved in the specific binding of galectin-4 to these compounds by modifying the conformation of these glycolipids as already observed by Iida-Tanaka and Ishizuka (2000).

GalNAcα-*O*-bn decreased the level of galactosylceramides and sulfatides. The inhibition of the synthesis of these glycosphingolipids is not surprising because the UDP-Gal required for galactosylceramide and sulfatide synthesis is mobilized by the inhibitor to produce different metabolites of GalNAcα-*O*-bn (Zanetta et al., 2000). From these results we conclude that despite its ability to interfere with *O*-glycosylation of glycoproteins, GalNAcα-*O*-bn exerts its inhibitory effect on apical transport mainly by inhibiting the synthesis of galactosylceramides and sulfatides and by blocking galectin-4 secretion. Most importantly, our data based on RNA silencing also demonstrate that galectin-4 directly participates in regulating apical transport. Previously, we have demonstrated that proteins assumed to be part of the apical delivery mechanism, syntaxin 3 and annexin XIIIb, also accumulated intracellularly after inhibitor treatment (Delacour et al., 2003). Similarly, annexin XIIIb was mislocalized in galectin-4–depleted cells (unpublished data). Thus, both apical cargo and apical machinery seem to depend on galectin-4 function. Galectin-4 could cross-link glycolipids to form raft platforms for apical sorting. Another common feature in GalNAcα-*O*-bn–treated and in galectin-4-KD cells is the lack of missorting of the apical cargo to the basolateral plasma membrane. This contrasts a number of earlier reports where inhibition of apical pathway led to measurable missorting to the basolateral pathway (Scheiffele et al., 1995; Keller and Simons, 1998). The level at which the apical pathway is affected may play a role. For example, a block at the level of TGN might still allow misloading of apical proteins for basolateral delivery but the fate of apical cargo might be different if the inhibition is exerted at a later step in the pathway. Therefore, an important issue that needs to be clarified is where does galectin-4 enter the biosynthetic pathway. We did observe galectin-4 in membrane vesicles derived from perforated HT-29 cells. Protease treatment demonstrated that galectin-4 was in the lumen of these vesicles that also labeled with antibodies against DPP-IV in immunoelectron microscopy. However, we do not know exactly where these vesicles derive from.

The route for apical delivery could involve direct delivery from the TGN but the transcytosis route over the basolateral membrane could also be used (Mostov et al., 2003; Nelson, 2003). Moreover, apical recycling endosomes have been implicated in apical traffic. Nevertheless, we assume that galectin-4 binding to sulfatides and galactosylceramides implicate lipid rafts in the apical delivery process. By binding to these raft constituents galectin-4 would cross-link rafts to form raft clusters, postulated to build up the membrane microdomains that bud off to generate transport carriers (Schuck and Simons, 2004). Because raft partitioning alone is not a sufficient criteria securing for apical delivery one would have to assume that also other scaffolding mechanisms (potentially also including direct lectin sorting of *N*- and *O*-glycosylated proteins) participate to ensure specific apical delivery. Galectin-4 could recycle from the apical membrane raft bound to facilitate raft clustering during biosynthetic transport. Perhaps we have to envisage apical sorting as a maturation process where the biosynthetic membrane carriers meet with endocytic carriers bringing back the machinery from the apical transport that will be required for proper apical delivery. We have perhaps been too strict in our attempts to define stations in an extremely dynamic network of membrane trafficking. Future work will have to define how this post-Golgi circuit operates and what path apical cargo takes and where it meets with recycling machinery.

Materials and methods

Materials

Recombinant rat galectin-4 CRD domains (C-G4-GST or N-G4-GST using pGEX-2T expression vectors; provided by K. Wasano, Kyushu University, Fukuoka, Japan) were prepared as previously described (Wasano and Hirakawa, 1999; Wu et al., 2002).

Antibodies

For Western blotting experiments, pAbs against porcine galectin-4 and against human annexin XIII (Intestinal Specific Antigen; Wice and Gordon, 1992) and rat mAb against human DPP-IV (4H3) were gifts from E.M. Danielsen (University of Copenhagen, Denmark), J. Gordon (Washington University School of Medicine, St. Louis, MO), and D. Massey (Gorvel et al., 1991), respectively. For morphological and co-immunoprecipitation experiments, a pAb against human galectin-4 was used (raised as described previously [Nagy et al., 2003] and checked for lack of cross-reactivity against other members of the galectin family [i.e., galectins-1, -2, -3, -5, -7, and -8]), and an mAb against human DPP-IV (HBB 3/775/42; HP Hauri, Biocenter of the University of Basel). Mouse mAbs against MUC1 (214D4), CEA (517), and LAMP2 (AC17) and ST3Gal I (4B10) were gifts from J. Hilkens (The Netherlands Cancer Institute, Amsterdam, Netherlands), A. Le Bivic (IBDM, Marseille, France) and U. Mandel (School of Dentistry, Copenhagen, Den-

mark), respectively. Mouse mAbs against human DPP-IV (M-A261) and human E-cadherin (HECD-1) were purchased from BD Biosciences and Takara. Rabbit pAbs against GST-fusion proteins and calnexin were obtained from Upstate Biotechnology and Santa Cruz Biotechnology, Inc.

Cell culture

HT-29 clone 5M12 cells were cultured as previously described (Delacour et al., 2003). GalNAcα-*O*-bn was used at the concentration of 2 mM for 10 d.

Isolation and characterization of DRMs

DRMs were isolated from a total membrane fraction after treatment with 1% Triton X-100 at 4°C (Fiedler et al.,1993).

Vesicle isolation from perforated cells

TGN-derived vesicles were isolated according to the procedure described by Wandinger-Ness et al. (1990). The absence of ER contamination in the vesicle preparation was checked by Western blotting with an antibody against calnexin (Fig. S4, available at http://www.jcb.org/cgi/content/full/jcb.200407073/DC1).

Single and double labellings were performed using rabbit anti–galectin-4 antibody and mouse anti–DPP-IV antibody (Scheiffele et al., 1998). Trypsinization was performed with trypsin (0.1 μg/ml) for 30 min at 37°C. Detergent extractability was analyzed by sequential detergent extraction at 4°C and 37°C according to the procedure of Braccia et al. (2003).

Proteomic analysis

2-D gels and MALDI-TOF mass spectrometry analyses were performed as previously described (Delacour et al., 2003) and silver-stained (Gharahdaghi et al., 1999).

Lipid extraction and analysis

Lipids were analyzed by HPTLC according to Vitiello and Zanetta (1978) for neutral lipids, and to Zanetta et al. (1980) for gangliosides and then by GC/MS as heptafluorobutyrate derivates (Zanetta et al., 1999; Pons et al., 2000, 2002). Glycolipids were isolated from human sciatic nerve (Zanetta et al., 1999; Pons et al., 2002).

Separation of cytosol and membranes by saponin treatment

Cells were incubated twice for 30 min at 4°C in PBS containing 2 mg/ml saponin, 5 mM EDTA, and protease inhibitors. Supernatants were collected and cells were then lysed in warm RIPA buffer (0.1 M Tris-HCl, pH 8.0, 1 M NaCl, 10 mM EDTA, 1% vol/vol Triton X-100, 5% wt/vol sodium desoxycholate, 1% vol/vol SDS, protease inhibitors).

Confocal microscopy

Confocal microscopy was performed according to Gouyer et al. (2001) with pAb anti–galectin-4 (1/50), mAbs anti–DPP-IV (1/100), anti-MUC1 (1/3), anti-CEA (1/500), anti–E-cadherin (1/500), anti–lysosome-associated membrane protein 2 (1/500), and anti-ST3Gal I (1/4) using a DMIRBE microscope (model TCS-NT; Leica) with a 63× 1.32 Plan-Apochromat oil-immersion objective lens. Acquisition was performed using Power Scan software (Leica) and processed with Adobe Photoshop 5.0.

For trypsinization on living cells, the cells were treated with 0.1 μg/ml trypsin for 10 min at 4°C. For detergent extraction on living cells, the cells were incubated for 2 min in 10 mM Hepes, pH 7.4, 1 mM $CaCl_2$, 1% Triton X-100, at 4 or 37°C.

Co-immunoprecipitation

Cells were lysed in a nondenaturing buffer (25 mM Tris-HCl, pH 7.5, 1 mM EDTA, 1 mM EGTA, 100 mM NaCl, 1% Triton X-100, 0.5% NP-40, and protease inhibitors) at RT. Immunoprecipitation was carried out with anti–galectin-4 antibody and magnetic beads.

Western blot analysis

The samples were processed as previously described (Gouyer et al., 2001).

Protein-lipid overlay assay

Galactosyl-ceramides and sulfatides from human sciatic nerve were separated by chromatography on aluminium-backed silica gel thin layer. Binding of galectin-4 domains was studied as described previously (Thomas et al., 2001) in the presence of 0.3% periodate-treated BSA (Glass et al., 1981).

Inhibition of galectin-4 gene expression by retroviral-mediated RNAi

Galectin-4-KD HT-29 5M12 cells were generated by using a retrovirus-mediated RNAi system as described previously (Schuck et al., 2004). In brief, oligonucleotides encoding shRNAs directed against galectin-4 mRNA were designed according to recommendations described in Schuck et al. (2004). The RNAi hairpin was designed to target human galectin-4 sequence 508–528:GGACATTGCCATCAACAGCTG. 0.4×10^6 cells were seeded into a well of 6-well plate. On the next day, cells were infected with either a control virus (without a hairpin insert) or a Gal-4-KD-virus in the presence of 8 μg/ml polybrene (hexadimethrine bromide; Fluka). Cells were incubated at 37°C overnight and infection was repeated twice with a fresh batch of virus. 1 d after the last infection, transduced cells were selected in the presence of 4 μg/ml puromycin for 3 d. 1 wk after selection, the KD efficiency was analyzed by quantitative RT-PCR and Western blotting.

Pulse-chase and transport assays

Cells were grown on Transwells (Costar Data Packaging) until day 10 and processed for radiolabeling and cell surface biotinylation (Le Bivic et al., 1989). Quantitation was performed with Claravision.

Online supplemental material

Fig. S1 shows NMR spectroscopy analysis of the galectin-4 ligands, i.e., sulfatide and galactosylceramide. Fig. S2 shows the three galectin-4 RNAi constructs tested: effect on galectin-4 expression and MUC1 localization. Fig. S3 shows the biosynthetic transport of basolateral and apical variants of ts045 VSV-G-GFP-fusion proteins in control and galectin-4 KD cells. Fig. S4 shows the absence of ER contaminations in the post-Golgi vesicle preparations of HT-29 5M12 cells. Further comments on the data can be found in the legends. Online supplemental material is available at http://www.jcb.org/cgi/content/full/jcb.200407073/DC1.

We thank Dr E.M. Danielsen, Dr D. Massey and Dr U. Mandel for their gift of antibodies. We thank Dr. K. Wasano for the gift of expression vector of recombinant rat galectin-4. Confocal microscopy and qRT-PCR were carried out in the IFR114. MALDI-TOF spectrometry was carried out in CNRS UMR 8525, Lille (Pr C. Serghereart). We thank C. Richet and M.J. Dejonghe for technical assistance, Drs. D. Belaiche and N. Sergeant for her help in proteomic analysis, Dr. Amena Ben Younes, Brigitte Hemon, and Anne Loyens for her help in electron microscopy experiments.

This work was supported by a grant from Association pour la Recherche contre le Cancer (5687). A. Manninen is a recipient of EMBO long term fellowship.

Submitted: 13 July 2004
Accepted: 15 March 2004

References

Alfalah, M., R. Jacob, U. Preuss, K.P. Zimmer, H. Naim, and H.Y. Naim. 1999. O-linked glycans mediate apical sorting of human intestinal sucrase-isomaltase through association with lipid rafts. *Curr. Biol.* 9:593–596.

Alfalah, M., R. Jacob, and H.Y. Naim. 2002. Intestinal dipeptidyl peptidase IV is efficiently sorted to the apical membrane through the concerted action of N- and O-glycans as well as association with lipid microdomains. *J. Biol. Chem.* 277:10683–10690.

Benting, J.H., A.G. Rietveld, and K. Simons. 1999. *N*-glycans mediate the apical sorting of a GPI-anchored, raft-associated protein in Madin-Darby canine kidney cells. *J. Cell Biol.* 146:313–320.

Braccia, A., M. Villani, L. Immerdal, L.L. Niels-Christiansen, B.T. Nystrom, G. Hansen, and E.M. Danielsen. 2003. Microvillar membrane microdomains exist at physiological temperature. Role of galectin-4 as lipid raft stabilizer revealed by "superrafts". *J. Biol. Chem.* 278:15679–15684.

Brown, D.A., and J.K. Rose. 1992. Sorting of GPI-anchored proteins to glycolipid-enriched membrane subdomains during transport to the apical cell surface. *Cell.* 68:533–544.

Byrd, J.C., R. Dahiya, J. Huang, and Y.S. Kim. 1995. Inhibition of mucin synthesis by benzyl-alpha-GalNAc in KATO III gastric cancer and Caco-2 colon cancer cells. *Eur. J. Cancer.* 31A:1498–1505.

Danielsen, E.M., and B. van Deurs. 1997. Galectin-4 and small intestinal brush border enzymes form clusters. *Mol. Biol. Cell.* 8:2241–2251.

Delacour, D., V. Gouyer, E. Leteurtre, T. Ait-Slimane, H. Drobecq, C. Lenoir, O. Moreau-Hannedouche, G. Trugnan, and G. Huet. 2003. 1-benzyl-2-acetamido-2-deoxy-alpha-D-galactopyranoside blocks the apical biosynthetic pathway in polarized HT-29 cells. *J. Biol. Chem.* 278:37799–37809.

Delannoy, P., I. Kim, N. Emery, C. De Bolos, A. Verbert, P. Degand, and G. Huet. 1996. Benzyl-N-acetyl-alpha-D-galactosaminide inhibits the sialylation and the secretion of mucins by a mucin secreting HT-29 cell subpopulation. *Glycoconj. J.* 13:717–726.

Dunphy, J.L., G.J. Barcham, R.J. Bischof, A.R. Young, A. Nash, and E.N.T.

Meeusen. 2002. Isolation and characterization of a novel eosinophil-specific galectin released into the lungs in response to allergen challenge. *J. Biol. Chem.* 277:14916–14924.

Fiedler, K., and K. Simons. 1996. Characterization of VIP36, an animal lectin homologous to leguminous lectins. *J. Cell Sci.* 109:271–276.

Fiedler, K., T. Kobayashi, T.V. Kurzchalia, and K. Simons. 1993. Glycosphingolipid-enriched, detergent-insoluble complexes in protein sorting in epithelial cells. *Biochemistry.* 32:6365–6373.

Folsch, H., H. Ohno, J.S. Bonifacino, and I. Mellman. 1999. A novel clathrin adaptor complex mediates basolateral targeting in polarized epithelial cells. *Cell.* 99:189–198.

Fred Brewer, C. 2002. Binding and cross-linking properties of galectins. *Biochim. Biophys. Acta.* 1572:255–262.

Füllekrug, J., P. Scheiffele, and K. Simons. 1999. VIP36 localisation to the early secretory pathway. *J. Cell Sci.* 112:2813–2821.

Gharahdaghi, F., C.R. Weinberg, D.A. Meagher, B.S. Imai, and S.M. Mische. 1999. Mass spectrometric identification of proteins from silver-stained polyacrylamide gel: a new method for the removal of silver ions to enhance sensitivity. *Electrophoresis.* 20:601–605.

Glass, W.F., II, R.C. Briggs, and L.S. Hnilica. 1981. Use of lectins for detection of electrophoretically separated glycoproteins transferred onto nitrocellulose sheets. *Anal. Biochem.* 115:219–224.

Gorvel, J.P., A. Ferrero, L. Chambraud, A. Rigal, J. Bonicel, and S. Maroux. 1991. Expression of sucrase-isomaltase and dipeptidylpeptidase IV in human small intestine and colon. *Gastroenterology.* 101:618–625.

Gouyer, V., E. Leteurtre, P. Delmotte, W.F.A. Steelant, M.A. Krzewinski-Recchi, J.P. Zanetta, T. Lesuffleur, G. Trugnan, P. Delannoy, and G. Huet. 2001. Differential effect of GalNAcα-*O*-bn on intracellular trafficking in enterocytic HT-29 and Caco-2 cells: relation with the glycosyltransferase expression pattern. *J. Cell Sci.* 114:1455–1471.

Gray, C.A., D.L. Adelson, F.W. Bazer, R.C. Burghardt, E.N.T. Meeusen, and T.E. Spencer. 2004. Discovery and characterization of an epithelial-specific galectin in the endometrium that forms crystals in the trophectoderm. *Proc. Natl. Acad. Sci. USA.* 101:7982–7987.

Gut, A., F. Kappeler, N. Hyka, M.S. Balda, H.P. Hauri, and K. Matter. 1998. Carbohydrate-mediated Golgi to cell surface transport and apical targeting of membrane proteins. *EMBO J.* 17:1919–1929.

Hara-Kuge, S., A. Seko, O. Shimada, H. Tosaka-Shimada, and K. Yamashita. 2004. The binding of VIP36 and α-amylase in the secretory vesicles via high-mannose type glycans. *Glycobiology.* 14:739–744.

Huang, J., J.C. Byrd, W.H. Yoor, and Y.S. Kim. 1992. Effect of benzyl-α-GalNAc, an inhibitor of mucin glycosylation, on cancer-associated antigens in human colon cancer cells. *Oncol. Res.* 4:507–515.

Huet, G., S. Hennebicq-Reig, C. de Bolos, F. Ulloa, T. Lesuffleur, A. Barbat, V. Carriere, I. Kim, F.X. Real, P. Delannoy, and A. Zweibaum. 1998. GalNAcα-*O*-benzyl inhibits NeuAcα2-3 glycosylation and blocks the intracellular transport of apical glycoproteins and mucus in differentiated HT-29 cells. *J. Cell Biol.* 141:1311–1322.

Hughes, R.C. 1999. Secretion of the galectin family of mammalian carbohydrate-binding proteins. *Biochim. Biophys. Acta.* 1473:172–185.

Iida-Tanaka, N., and I. Ishizuka. 2000. Complete 1H and 13C NMR assignment of mono-sulfated galactosylceramides with four types of ceramides from human kidney. *Carbohydr. Res.* 324:218–222.

Ideo, H., A. Seko, T. Ohkura, K.L. Matta, and K. Yamashita. 2002. High-affinity binding of recombinant human galectin-4 to $SO_3^- \rightarrow 3Gal\beta1 \rightarrow 3GalNAc$ pyranoside. *Glycobiology.* 12:199–208.

Jacob, R., M. Alfalah, J. Grünberg, M. Obendorf, and H.Y. Naim. 2000. Structural determinants required for apical sorting of an intestinal brush-border membrane protein. *J. Biol. Chem.* 275:6566–6572.

Keller, P., and K. Simons. 1998. Cholesterol is required for surface transport of influenza virus hemagglutinin. *J. Cell Biol.* 140:1357–1367.

Le Bivic, A., F.X. Real, and E. Rodrigues-Boulan. 1989. Vectorial targeting of apical and basolateral plasma membrane proteins in a human adenocarcinoma epithelial cell line. *Proc. Natl. Acad. Sci. USA.* 86:9313–9317.

Leffler, H., S. Carlsson, M. Hedlund, Y. Qian, and F. Poirier. 2004. Introduction to galectins. *Glycoconj. J.* 19:433–440.

Lipardi, C., L. Nitsch, and C. Zurzolo. 2000. Detergent-insoluble GPI-anchored proteins are apically sorted in fischer rat thyroid cells, but interference with cholesterol or sphingolipids differentially affects detergent insolubility and apical sorting. *Mol. Biol. Cell.* 11:531–542.

Matter, K., and I. Mellman. 1994. Mechanisms of cell polarity: sorting and transport in epithelial cells. *Curr. Opin. Cell Biol.* 6:545–554.

Monlauzeur, L., L. Breuza, and A. Le Bivic. 1998. Putative *O*-glycosylation sites and a membrane anchor are necessary for apical delivery of the human neurotrophin receptor in Caco-2 cells. *J. Biol. Chem.* 273:30263–30270.

Mostov, K.E., M. Verges, and Y. Altschuler. 2000. Membrane traffic in polarized epithelial cells. *Curr. Opin. Cell Biol.* 12:483–490.

Mostov, K., T. Su, and M. ter Beest. 2003. Polarized epithelial membrane traffic: conservation and plasticity. *Nat. Cell Biol.* 5:287–293.

Nagy, N., H. Legendre, O. Engels, S. André, H. Kaltner, K. Wasano, Y. Zick, J.C. Pector, C. Decaestecker, H.J. Gabius, et al. 2003. Refined prognostic evaluation in colon carcinoma using immuno-histochemical galectin fingerprinting. *Cancer.* 97:1849–1858.

Nakatsu, F., and H. Ohno. 2003. Adaptor protein complexes as the key regulators of protein sorting in the post-Golgi network. *Cell Struct. Funct.* 28:419–429.

Nickel, W. 2003. The mystery of nonclassical protein secretion. *Eur. J. Biochem.* 270:2109–2119.

Nelson, W.J. 2003. Adaptation of core mechanisms to generate cell polarity. *Nature.* 422:766–774.

Oda, Y., J. Herrmann, M.A. Gitt, C.W. Turck, A.L. Burlingame, S.H. Barondes, and H. Leffler. 1993. Soluble lactose-binding lectin from rat intestine with two different carbohyrate-binding domains in the same peptide chain. *J. Biol. Chem.* 268:5929–5939.

Pons, A., J. Popa, J. Portoukalian, J. Bodennec, D. Ardail, O. Kol, M.J. Martin-Martin, P. Hueso, P. Timmerman, Y. Leroy, and J.P. Zanetta. 2000. Single step GC/MS analysis of glycolipid constituents as heptafluorobutyrate with a special reference to the lipid portion. *Anal. Biochem.* 284:201–216.

Pons, A., P. Timmerman, Y. Leroy, and J.P. Zanetta. 2002. GC/MS analysis of human skin long-chain bases as heptafluorobutyrate derivatives. *J. Lipid Res.* 43:794–804.

Scheiffele, P., J. Peranen, and K. Simons. 1995. N-glycans as apical sorting signals in epithelial cells. *Nature.* 378:96–98.

Scheiffele, P., P. Verkade, A.M. Fra, H. Virta, K. Simons, and E. Ikonen. 1998. Caveolin-1 and -2 in the exocytic pathway of MDCK cells. *J. Cell Biol.* 140:795–806.

Schuck, S., and K. Simons. 2004. Polarized sorting in epithelial cells: Raft clustering and the biogenesis of the apical membrane. *J. Cell Sci.* 117:5955–5964.

Schuck, S., A. Manninen, M. Honsho, J. Füllekrug, and K. Simons. 2004. Generation of single and double knockdowns in polarized epithelial cells by retrovirus-mediated RNA interference. *Proc. Natl. Acad. Sci. USA.* 101:4912–4917.

Simons, K., and E. Ikonen. 1997. Functional rafts in cell membranes. *Nature.* 387:569–572.

Thomas, C.C., S. Dowler, M. Deak, D.R. Alessi, and D.M.F. Aalten. 2001. Crystal structure of the phosphatidylinositol 3,4-biphosphate-binding pleckstrin homology (PH) domain of tandem PH-domain-containing protein 1 (TAPP1): molecular basis of lipid specificity. *Biochem. J.* 358:287–294.

Vitiello, F., and J.P. Zanetta. 1978. Thin-layer chromatography of phospholipids. *J. Chromatogr.* 166:637–640.

Wandinger-Ness, A., M.K. Bennett, C. Antony, and K. Simons. 1990. Distinct transport vesicles mediate the delivery of plasma membrane proteins to the apical and basolateral domains of MDCK cells. *J. Cell Biol.* 111:987–1000.

Wasano, K., and Y. Hirakawa. 1999. Two domains of rat galectin-4 bind to distinct structures of the intercellular borders of colorectal epithelia. *J. Histochem. Cytochem.* 47:75–82.

Wice, B.M., and J.L. Gordon. 1992. A strategy for isolation of cDNAs encoding proteins affecting human intestinal epithelial cell growth and differenciation: characterization of a novel gut-specific N-myristoylated annexin. *J. Cell Biol.* 116:405–422.

Wu, A.M., J.H. Wu, M.S. Tsai, J.H. Liu, S. André, K. Wasano, H. Kaltner, and H.J. Gabius. 2002. Fine specificity of the domain-I of recombinant tandem-repeat-type galectin-4 from rat gastrointestinal tract (G4-N). *Biochem. J.* 367:653–664.

Yeaman, C., A.H. Le Gall, A.N. Baldwin, L. Monlauzeur, A. Le Bivic, and E. Rodriguez-Boulan. 1997. The *O*-glycosylated stalk domain is required for apical sorting of neurotrophin receptors in polarized MDCK cells. *J. Cell Biol.* 139:929–940.

Zanetta, J.P., F. Vitiello, and G. Vincendon. 1980. Gangliosides from rat cerebellum: demonstration of a considerable heterogeneity using a new solvent for thin-layer chromatography. *Lipids.* 15:1055–1061.

Zanetta, J.P., P. Timmerman, and Y. Leroy. 1999. Gas-liquid chromatography of the heptafluorobutyrate derivatives of the *O*-methyl glycosides on capillary columns: a method for the quantitative determination of the monosaccharide composition of glycoproteins and glycolipids. *Glycobiology.* 9:255–266.

Zanetta, J.P., V. Gouyer, E. Maes, A. Pons, B. Hemon, A. Zweibaum, P. Delannoy, and G. Huet. 2000. Massive *in vitro* synthesis of tagged oligosaccharides in 1-benzyl-2-acetamido-2-deoxy-α-D-galactopyranoside treated HT-29 cells. *Glycobiology.* 10:565–575.